



## Generation of metal composition gradients by means of bipolar electrodeposition

Gwendoline Tisserant, Zahra Fattah, Cédric Ayela, Jérôme Roche, Bernard Plano, Dodzi Zigah, Bertrand Goudeau, Alexander Kuhn, Laurent Bouffier

### ► To cite this version:

Gwendoline Tisserant, Zahra Fattah, Cédric Ayela, Jérôme Roche, Bernard Plano, et al.. Generation of metal composition gradients by means of bipolar electrodeposition. *Electrochimica Acta*, 2015, 179, pp.276-281. 10.1016/j.electacta.2015.03.102 . hal-02049662

**HAL Id: hal-02049662**

**<https://hal.science/hal-02049662>**

Submitted on 26 Feb 2019

**HAL** is a multi-disciplinary open access archive for the deposit and dissemination of scientific research documents, whether they are published or not. The documents may come from teaching and research institutions in France or abroad, or from public or private research centers.

L'archive ouverte pluridisciplinaire **HAL**, est destinée au dépôt et à la diffusion de documents scientifiques de niveau recherche, publiés ou non, émanant des établissements d'enseignement et de recherche français ou étrangers, des laboratoires publics ou privés.




## Open Archive Toulouse Archive Ouverte (OATAO)

OATAO is an open access repository that collects the work of Toulouse researchers and makes it freely available over the web where possible

This is an author's version published in: <http://oatao.univ-toulouse.fr/21899>

**Official URL:** <https://doi.org/10.1016/j.electacta.2015.03.102>

### **To cite this version:**

Tisserant, Gwendoline and Fattah, Zahra and Ayela, Cédric and Roche, Jérôme  and Plano, Bernard and Zigah, Dodzi and Goudeau, Bertrand and Kuhn, Alexander and Bouffier, Laurent *Generation of metal composition gradients by means of bipolar electrodeposition*. (2015) *Electrochimica Acta*, 179. 276-281. ISSN 0013-4686

Any correspondence concerning this service should be sent  
to the repository administrator: [tech-oatao@listes-diff.inp-toulouse.fr](mailto:tech-oatao@listes-diff.inp-toulouse.fr)

# Generation of metal composition gradients by means of bipolar electrodeposition

Gwendoline Tisserant<sup>a,b</sup>, Zahra Fattah<sup>c</sup>, Cédric Ayela<sup>d,e</sup>, Jérôme Roche<sup>a,b</sup>, Bernard Plano<sup>d,e</sup>, Dodzi Zigah<sup>a,b</sup>, Bertrand Goudeau<sup>a,b</sup>, Alexander Kuhn<sup>a,b</sup>, Laurent Bouffier<sup>a,b,\*</sup>

<sup>a</sup> Univ. Bordeaux, ISM, UMR 5255, F-33400 Talence, France

<sup>b</sup> CNRS, ISM, UMR 5255, F-33400 Talence, France

<sup>c</sup> Univ. of Duhok, Zakho Street 38, 1006 AJ Duhok, Kurdistan Region, Iraq

<sup>d</sup> Univ. Bordeaux, IMS, UMR 5218, F-33400 Talence, France

<sup>e</sup> CNRS, IMS, UMR 5218, F-33400 Talence, France

## ARTICLE INFO

### Keywords:

Bipolar electrochemistry  
Metal electrodeposition  
Chemical gradients  
Asymmetric surfaces

## ABSTRACT

Bipolar electrochemistry is an unconventional technique that currently encounters a renewal of interest due to modern applications in the fields of analytical chemistry or materials science. The approach is particularly relevant for the preparation of asymmetric objects or surfaces such as *Janus* particles for example. Bipolar electrochemistry allows spatially controlled deposition of various layers from electroactive precursors, selectively at one side of a bipolar electrode. We report here the concomitant cathodic deposition of up to three different metals at the same time in a single experiment. The deposits were characterized by optical and electron microscopy imaging as well as profilometry and energy dispersive X-ray spectroscopy. As a result, the deposited layer is composed of several areas exhibiting both a composition and a thickness gradient. Such a variation directly modifies the optical and electronic properties alongside the surface and gives access to the design of composite surfaces exhibiting a visual gradient feature.

## 1. Introduction

The synthesis of material gradients is an essential topic of research related to the control of various physico-chemical properties alongside an object or a surface. Nowadays, gradients are employed in many technological applications while several electrochemical approaches have been developed to fabricate such structures [1].

Bipolar electrochemistry (BPE) has been described as an original approach for the formation of surface gradients on conductive substrates [2–6]. The general idea is to control the electrochemical reactivity on a conducting surface immersed in a low conductivity solution and positioned between two feeder electrodes by applying an external electric field. The potential of the solution evolves linearly across the solution, but since the conducting object is equipotential, an interfacial difference of polarization arises along the object. When the external field is of

sufficient amplitude, it is possible to carry out electrochemical reactions, namely a reduction at the side facing the feeder anode and an oxidation at the extremity in front of the feeder cathode [7–10]. An important point is that the polarization potential varies alongside the bipolar electrode meaning that there is a driving force gradient established parallel to the electric field lines. This approach was first used to prepare molecular gradients on a gold surface based on the reductive desorption of thiol-based self-assembled monolayers [2]. The authors also studied in details the potential distribution on a bipolar electrode [3]. Another important contribution in the field has been exemplified with the bipolar patterning of conducting polymers that can be electrogenerated from monomers on a bipolar electrode [4]. It has been demonstrated that the polarization gradient is responsible for a variation of doping alongside the surface, and therefore leads to a direct modulation of the resulting electronic properties [4–6]. An alternative way to promote a molecular gradient was also demonstrated by the grafting of diazonium salts on a carbon substrate by means of spatially controlled electroreduction [11].

Metal electrodeposition is also a very classic approach to prepare asymmetric objects or surfaces [12–20]. Bimetallic

\* Corresponding author.

E-mail address: laurent.bouffier@enscbp.fr (L. Bouffier).

composition gradients based on Ag–Au alloys formed on a bipolar electrode have been reported and characterized by surface-enhanced Raman spectroscopy [21]. The formation of one-dimensional chemical composition gradients of CdS on gold surfaces was equally achieved [22]. Besides the composition gradients, a recent effort has been made to tune the morphology of the deposit in order to control precisely surface wettability [23]. A last example is also the fabrication of arrays of TiO<sub>2</sub> nanotube (NT) gradients by means of bipolar anodization [24]. Such an approach allows screening of the optimum NTs length to reach an optimized photocurrent response in dye-sensitized solar cells.

This recent interest in the control of composition gradients by means of BPE stimulated us to investigate the surface modification using a combination of up to three different metal precursors. Simultaneous bi-metallic deposition has been already reported [21], but to the best of our knowledge, a tri-metallic composite gradient generated by BPE has not been reported so far. The experiments have been carried out with three specific metals that were already deposited independently under BPE conditions [19,25,26] but such an approach is not restricted to such a specific choice of metals.

## 2. Experimental Section

**Chemicals:** All chemicals were used as received. Copper(II) sulfate anhydrous (98%) was purchased from Alfa Aesar. Nickel(II) sulfate hexahydrate (>99.9%) and Zinc(II) sulfate monohydrate (>99.9%) were purchased from Sigma Aldrich. Solutions were prepared using Milli-Q water (resistivity = 18.2 MΩ cm). The gold surfaces (size 5 × 5 mm<sup>2</sup>) with a 360 nm-thick metal layer were purchased from ACM (78640 Villiers, France). Prior to be used as bipolar electrodes, the surfaces were cleaned with Piranha solution (*Caution: Piranha solution is very dangerous, being both strongly acidic and also a strong oxidizer*) containing 25% H<sub>2</sub>O<sub>2</sub> and 75% H<sub>2</sub>SO<sub>4</sub>; washed with water and ethanol.

**Instrumentation:** During BPE experiments, the electric field was applied with a high power supply from Keithley (Electrometer model 6517B). Optical images were recorded with a MacroScope Z16 APO from Leica equipped with an objective (×0.8), a quarter-wave plate and a DFC295 camera. SEM images were collected with a Hitachi microscope (TM-1000). Contact profilometry was performed with a Alpha-step IQ apparatus from KLA-Tencor. Energy-dispersive X-ray spectroscopy was recorded on a JEOL JSM 8100 SEM coupled with an EDX analysis module from OXFORD System (INCA Energy 250 with thermoelectrically cooled solid-state silicon drift detector (SDD) and pre-amplifier. MnKα resolution: 128 eV; CKα resolution: 67 eV and FKα resolution: 69 eV. Detection: From Be to Pu).

## 3. Results and Discussion

As briefly stated in the introduction, the principle of BPE is based on the difference of potential polarization established between the solution and the bipolar electrode. The electric field is applied across the solution by two feeder electrodes connected to an external power supply (Fig. 1A). The driving force (or maximum polarization voltage,  $\Delta V_{\max}$ ) is directly proportional to the electric field ( $E_{\text{tot}}$ ) and the length of the bipolar electrode ( $l$ ) according to the following Eq. (1):

$$\Delta V_{\max} = E_{\text{tot}} \times l$$

This means that the promotion of electrochemical reactions at the two opposite ends of a conducting object needs a  $\Delta V_{\max}$  value which is at least equal to the difference between the formal standard potentials of the two reactions. As a consequence, the size

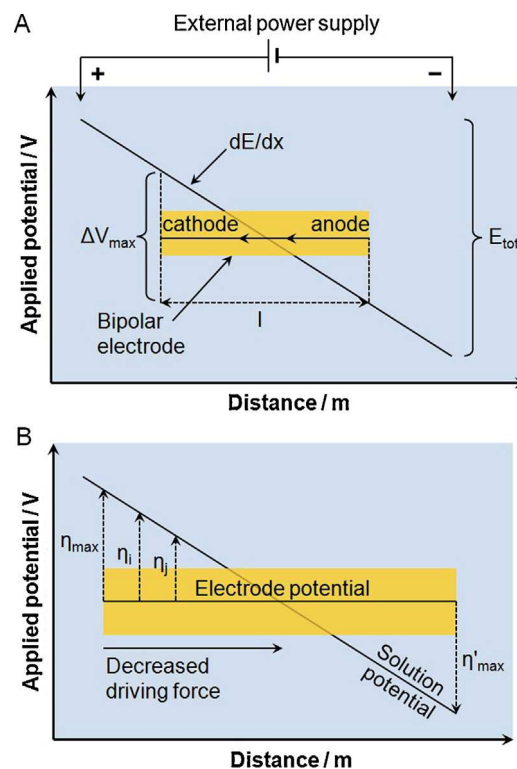


**Fig. 1.** Schematic representation of the principle of bipolar electrochemistry (A). The interfacial potential polarization between the solution and the bipolar electrode promotes bipolar reactions occurring at the two opposite sides. Scheme showing the decrease of the driving force alongside the bipolar electrode from the edge toward the middle (B), adapted from reference [9].

of the bipolar electrode is an intrinsic limitation because the smaller the electrode is, the higher the electric field has to be. Practically, the value of  $E_{\text{tot}}$  can vary from a couple of volts per centimeter in the case of macroscopic bipolar electrodes, up to a few kV/cm for microscale objects.

It is also important to mention that the polarization varies alongside the bipolar electrode, meaning that the highest overpotentials ( $\eta_{\max}$ ) are generated at the outermost extremities, or in other words a potential gradient is established along the bipolar electrode [27]. In the simplified symmetric case presented in Fig. 1B, the maximum anodic and cathodic polarization potentials are equal and, as a matter of fact, a decrease of the polarization potential is observed when moving from the edge towards the middle of the bipolar electrode ( $\eta_{\max} > \eta_i > \eta_j$ ). This is a major advantage of BPE when compared to conventional electrochemistry, for example in the case of electrodisolution or electrodeposition studies. Instead of studying the electrochemical reactivity at a single potential value, BPE allows screening a range of different thermodynamic conditions along the bipolar electrode in one single experiment [28].

In the present study, gold surfaces are chosen to carry out the electrodeposition of various metals by BPE. This kind of substrate is very appropriate because it is constituted by a glass slide covered with a 0.36  $\mu\text{m}$ -thick Au layer. The gold deposit is homogeneous, meaning that any further deposition will markedly modify the surface properties. Moreover, these surfaces have already been used for previous BPE studies [29].

A specific BPE cell was designed to perform the corresponding electrodeposition experiments, as illustrated in Fig. 2. It is made of a polydimethylsiloxane (PDMS) shaped cylinder where the right and left compartments accommodate a feeder electrode whereas the 1 cm-long central platform receives the square Au bipolar

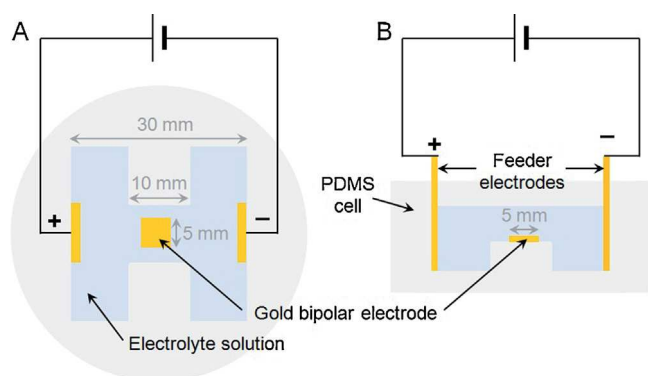


**Fig. 2.** Illustration of the electrochemical cell used to perform bipolar electrodeposition experiments: Top view (A) and side view (B), respectively.

electrode ( $5 \times 5 \text{ mm}^2$ ). The cell is filled with the electrolyte solution and the distance between the feeder electrodes is 3 cm. When a voltage is applied by the external power supply, the maximum possible polarization of the bipolar electrode is therefore a sixth part of the total voltage based on Eq. (1).

Initially, the deposition of a single metal layer on Au surfaces was studied. For that, three different metals, namely Cu, Ni and Zn were selected in order to achieve a deposition from precursors exhibiting contrasted reduction potentials. Indeed, the corresponding formal potentials are respectively  $E^\circ_{\text{Cu}^{2+}/\text{Cu}} = +0.34 \text{ V}$ ,  $E^\circ_{\text{Ni}^{2+}/\text{Ni}} = -0.25 \text{ V}$  and  $E^\circ_{\text{Zn}^{2+}/\text{Zn}} = -0.76 \text{ V}$  versus NHE. If one considers that the anodic reaction is the oxidation of water ( $E^\circ_{\text{O}_2/\text{H}_2\text{O}} = 1.23 \text{ V}$  versus NHE), the minimal polarization required between both ends of the bipolar electrode is  $\Delta V = 0.89 \text{ V}$ ,  $1.48 \text{ V}$  and  $1.99 \text{ V}$ , respectively.

All depositions have been performed by applying the electric field for 2 min. It has already been shown that much shorter times can also be used [30], but in the present case a thicker deposit was necessary in order to facilitate the visual characterization of the modified surfaces. An identical concentration of metal precursor (10 mM of  $\text{M}^{\text{II}}\text{SO}_4$ ) was used each time in order to reach a comparable ionic strength.

A selection of representative images of the modified surfaces are gathered in Fig. 3 in the case of copper (A–C), nickel (D,E) and zinc (F) deposition. These transmission optical images were recorded on a macroscope with a  $\times 0.8$  objective equipped with a polarizer to obtain a well-defined contrast. For Cu deposition, the electric field was varied between 2.5 and 6.3 V/cm. The corresponding deposition length was directly estimated from the optical images (Fig. 3A–C) and gathered in Table 1. As expected the zone where metal deposition occurs increases when applying larger electric field. Typically, the deposit length is about 0.15 mm at the lowest applied value (2.5 V/cm) whereas a large portion of the bipolar electrode is covered by Cu, typically up to 1.75 mm out of 5.0 mm at 4.7 V/cm (Fig. 3C). From the optical contrast, one can see that the Cu layer is not homogeneous on the whole surface, illustrating the establishment of a gradient of driving force along the bipolar electrode. This is especially true in the case of copper nucleation and growth which is known to be very sensitive to the local deposition conditions [31–34]. By comparison, Ni deposition requires at least 3.8 V/cm to be effective on the bipolar surface. The driving force was increased up to 6.3 V/cm and the length of the Ni deposit was found to range between 0.26 and 1.41 mm (Fig. 3D,E and Table 1). For a given value of the electric field, the area of Ni deposition is always smaller than the Cu one which is perfectly compatible with the difference of formal reduction potentials between Ni and Cu, respectively. In the case of Zn electroreduction, no visual deposit was observed with optical macroscopy (Fig. 3F) until the electric field value was raised to 9.4 V/cm. In fact, the calculation based on the formal redox potential predicts that a minimum electric field of 4 V/cm needs to be applied to drive the electrochemical reactions at the very edges of the bipolar electrode.

The experiments were carried out several times and even if the limit of deposition was sometimes well-aligned parallel to the feeder electrodes, a slight curvature was observed at several occasions (Fig. 3B, C and E). This was mostly observed in the case of Cu and can be explained as follows: (1) The Au plate was possibly not perfectly aligned with respect to the feeder electrodes. This could lead to inhomogeneous electric field lines because even a small tilt angle can result in a visible curvature for a large zone of

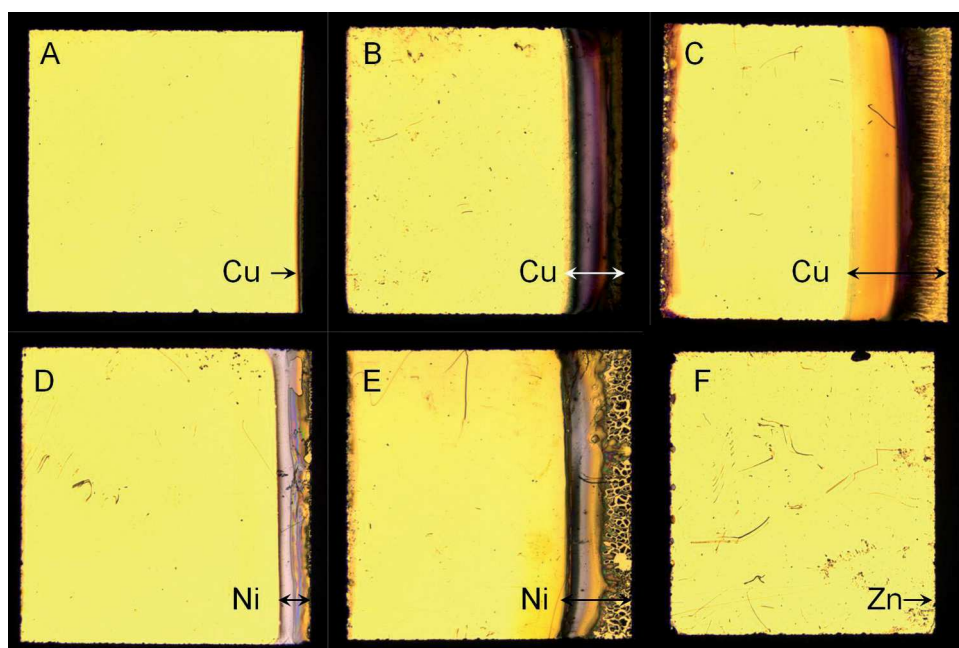


**Fig. 3.** Selection of optical images of a series of Au surfaces ( $5 \times 5 \text{ mm}^2$ ) modified with Copper (A–C), Nickel (D–E) or Zinc (F) by applying an electric field of 2.5 (A), 3.8 (B), 4.7 (C–F) or 5.6 V/cm (E) from 10 mM solutions of  $\text{CuSO}_4$ ,  $\text{NiSO}_4$  or  $\text{ZnSO}_4$ , respectively.



**Table 1**

BPE depositions are made with 10 mM solutions of metal sulfate during 120 s.

Electric Field (V/cm)	Deposit length (mm)		
	Cu	Ni	Zn
2.5	0.15	–	–
3.1	0.77	0	0
3.8	1.15	0.26	–
4.7	1.80	0.56	~0 <sup>c</sup>
5.6 <sup>a</sup>	–	1.15	–
6.3 <sup>a</sup>	2.10 <sup>b</sup>	1.41	~0 <sup>c</sup>
9.4 <sup>a</sup>	–	–	up to 0.2

<sup>a</sup> The applied electric field value deteriorated partially the anodic extremity of the gold plate,

<sup>b</sup> The deposition time was reduced to 10 s,

<sup>c</sup> The metal deposit is only observed at the very edge of the substrate (see Fig. 4).

deposition. (2) The applied electric field being larger than the threshold value to promote water splitting, pH gradients can equally establish at the vicinity of the bipolar electrode [35,36]. The inhomogeneous evolution and diffusion of these gradients with respect to ion migration can also modify locally the deposition conditions. The size ratio between the bipolar electrode and the electrochemical cell can also produce these effects. Indeed, a large bipolar electrode will be more prone to be affected by such inhomogeneous conditions.

The modified surfaces were also characterized at various magnifications by scanning electron microscopy (SEM). As already observed by optical imaging, the copper layer does not appear to be uniform over the deposition area as shown at a low magnification ( $\times 80$ ) in Fig. 4A. The images recorded at a higher magnification ( $\times 5000$ ) strongly support the presence of different thermodynamic deposition conditions. The Cu deposit observed in the zone close to the limit of deposition appears in the form of isolated clusters spread on the surface with a typical dimension of  $\sim 1 \mu\text{m}$  (Fig. 4A, left inset). On the other hand, the deposit imaged near the extremity of the gold plate reveals a Cu network where the previous clusters are larger and interconnected due to the higher driving force present in this area of the bipolar electrode (Fig. 4A, right inset). In contrast, the Ni layer seems to be more uniform as observed under the optical microscope. The high magnification SEM imaging reveals a thick deposit exhibiting a pronounced roughness (Fig. 4B). Finally, in the case of Zn for which the optical characterization was not fully conclusive, the deposit can be observed at the edge of the gold bipolar electrode with SEM. It appears as a small  $\sim 25 \mu\text{m}$ -large band of zinc (Fig. 4C). The corresponding inset shows the SEM image recorded with a zoom of  $\times 5000$  which evidences a very rough layer, comparable to the one observed in the case of Ni.

Based on this first series of experiments, the compromise value chosen for further deposition was  $4.7 \text{ V/cm}$ . It corresponds to a maximum polarization  $\Delta V = 2.35 \text{ V}$  for a  $5 \text{ mm}$ -long Au surface. Such a value allows a good discrimination between the thermodynamic thresholds for the individual deposition of each metal. Indeed, the corresponding driving force is large enough to drive either Cu or Ni deposition on a large area of the bipolar surface while it is just sufficient to promote the Zn deposition at the outermost edge of the bipolar electrode. It is noteworthy that a larger electric field value can also be chosen but is responsible for the degradation of the anodic edge through harsh oxidation conditions (typically observed between  $5.6$  and  $9.4 \text{ V/cm}$ ).

After this first series of monometallic deposition, the next step towards the preparation of more complex gradient structures consists in a single step BPE deposition from the combination of two or three metal precursors. In order to perform such a deposition, a total concentration of metal sulfate precursors of  $1 \text{ mM}$  was chosen. These experimental conditions are slightly

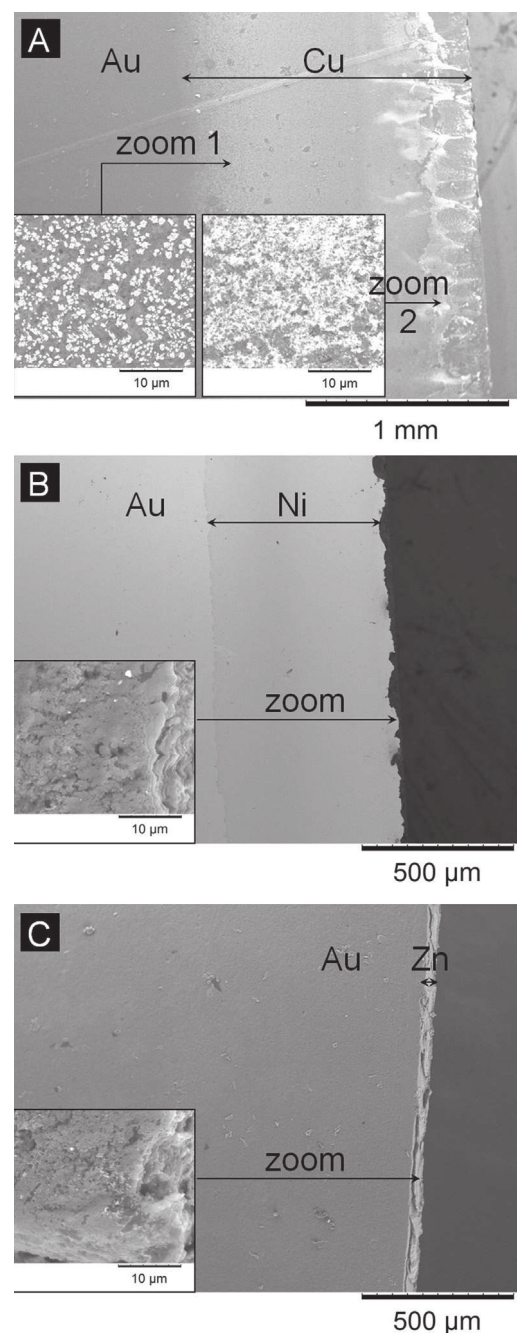


**Fig. 4.** Scanning electron microscopy images of Au surfaces modified by Copper (A), Nickel (B) or Zinc (C). Main images recorded at a magnification of  $\times 80$  (A) or  $\times 120$  (B, C); insets  $\times 5000$ .

different from the monometallic deposition because the individual concentration of each metal salt was lower ( $2 \times 0.5 \text{ mM}$  in the case of a bi-metallic deposition and  $3 \times 0.33 \text{ mM}$  for a tri-metallic deposition). However, such conditions maintain a comparable ionic strength, thus allowing the comparison of different experiments, because a change in ionic strength does influence the effective current flowing across the bipolar electrode by changing the bypass current across the solution [7]. Two bimetallic gradient surfaces were investigated with the concomitant electrodeposition of either Cu or Ni in the presence of Zn. In presence of copper and zinc salts, the corresponding optical characterization shows a clear deposition zone where Cu metal dominates ( $1.7 \text{ mm}$ ) whereas the deposit localized at the edge

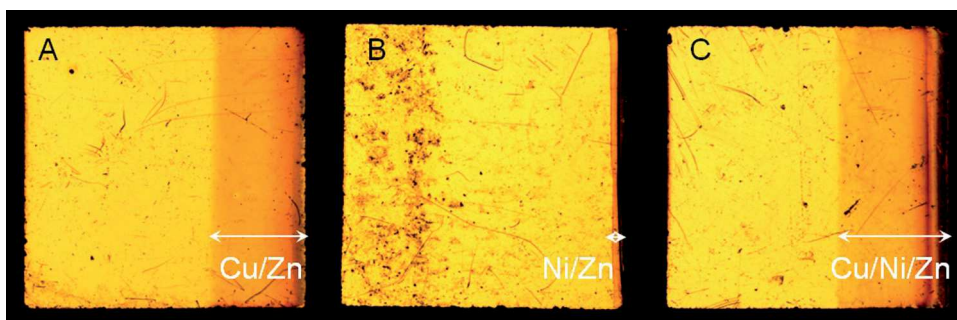


**Fig. 5.** Optical images of a series of Au surfaces ( $5 \times 5 \text{ mm}^2$ ) modified with Cu and Zn (A), Ni and Zn (B) or Cu, Ni and Zn (C) by applying an electric field of 4.7 V/cm from 1 mM solutions containing  $\text{CuSO}_4$ ,  $\text{NiSO}_4$  and/or  $\text{ZnSO}_4$ , respectively.

appears thicker (0.2 mm) which could be assigned to the presence of a zinc layer (Fig. 5A). In comparison the Ni/Zn co-deposit is located at the close proximity of the bipolar electrode edge (0.2 to 0.3 mm). However, two zones can be easily distinguished based on a variation of the optical index (Fig. 5B). Compared to the monometallic depositions, the bimetallic experiments result in a modification of the deposition area which could be explained to some extent by the lower concentration of each individual metal salt. In the case of a tri-metallic mixture, the main zone corresponding to the Cu deposit stretches as far as 1.8 mm whereas a series of marked stripes are clearly visible at the outer part of the layer (Fig. 5C). This gradient structure is due to a metal composition gradient combined with a variation of thickness.

The deposits have also been studied by using a contact profilometer (data not shown). Almost all the surfaces were consistently modified with metal layers exhibiting typically up to 100–200 nm thickness except the zinc deposit which was not measurable due to its localization at the very edge of the gold surface (Figure 3F and 4C). The copper deposits are thicker and less regular indicated by the corresponding profilometer data exhibiting a larger fluctuation. The single copper deposit has a thickness

ranging between 130 and 150 nm at the edge whereas the Cu/Zn co-deposit is slightly thicker (up to 200 nm). By comparison, the nickel layer is ~70 to 100 nm-thick and the Ni/Zn co-deposit shows a more pronounced variation between 50 and 100 nm. Finally, the trimetallic layer composed of Cu, Ni and Zn is also rather thick with a maximum value around ~180 nm. This series of results reveals that the thickness is fairly consistent from one layer to another but more importantly the nature of the metal strongly affects the roughness factor of each deposit, particularly in the case of copper.

Besides optical or electronic imaging, the chemical composition of the tri-metallic deposit was investigated by collecting energy dispersive X-ray (EDX) spectroscopy data. EDX spectra recorded at several positions on the surface clearly reveal the evolution of the chemical composition. Outside of the deposition zone, exclusively Au is detected whereas the presence of Cu, Ni and Zn appears sequentially while moving alongside the deposited layer. A SEM image of the modified surface and the corresponding chemical EDX mapping are gathered in Fig. 6. One can note that there is a steady drift in intensity along the surface which starts consistently where the first metal deposit appears. This is simply due to the fact that the signal corresponding to copper metal dominates the EDX

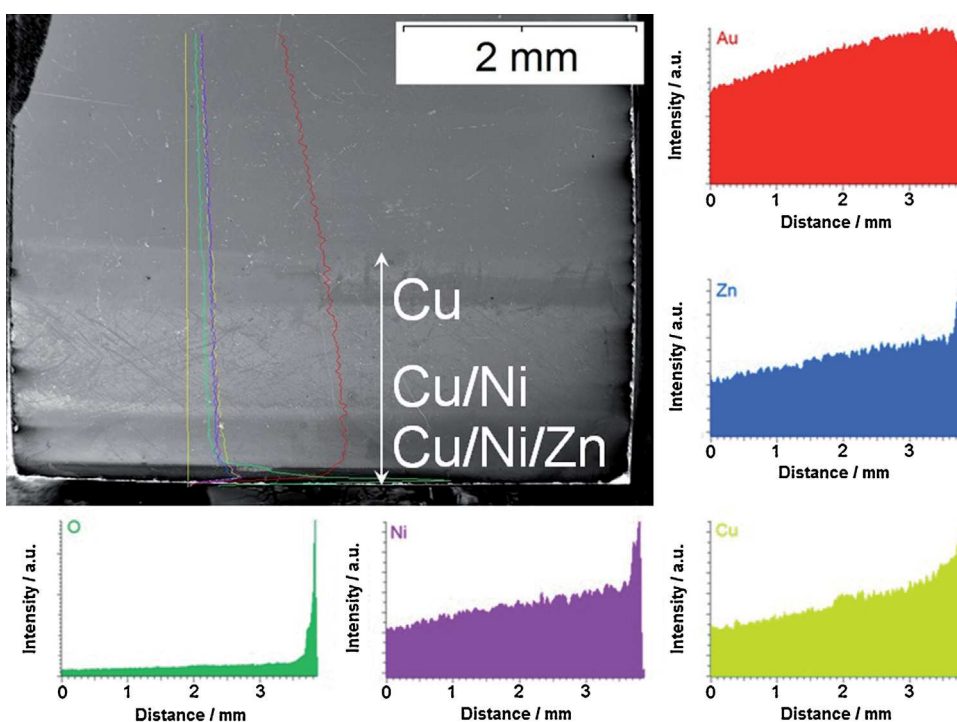


**Fig. 6.** Scanning electron microscopy image of the Au surface modified simultaneously by Cu, Ni and Zn. Insets: Energy dispersive X-ray spectroscopy mapping recorded alongside the modified bipolar electrode. N.B.: Intensities are given in arbitrary unit.

response and complicates the deconvolution of the signals assigned to the other metals. Therefore, a fully quantitative analysis is not possible but a rather qualitative trend can be revealed instead. As expected, the intensity corresponding to the Au signal appears everywhere on the surface. This signal is notably lower at the anodic part of the bipolar electrode. This is probably due to a slight mechanical deterioration of either the Cr/Ni underlayer or the gold layer itself due to strong water oxidation. Copper is the first metal which is detected at the limit between the bare surface and the deposit. Moreover, the intensity of this signal increases gradually when moving towards the cathodic extremity of the bipolar electrode. Then, Ni and Zn are detected gradually, especially at the edge of the surface. It is also noticeable that the Oxygen content is markedly higher at the edge and this is probably due to the pH gradient established at the vicinity of the bipolar electrode. Indeed, the applied electric field promotes not only the metal salts electroreduction but also the reduction of protons. This affects locally the pH which becomes more basic and could possibly shift the stability domain (Potential/pH) from pure metals to other forms. Therefore, it is believed that such an increase of the oxygen content reflects local changes in the composition of the deposit. Even if metals are mainly deposited, it is not excluded that oxides or hydroxides are also present in the layer. Moreover, partial oxidation of Cu metal can also occur *a posteriori*, especially on the top part of the deposit.

#### 4. Conclusion

The modification of a flat gold surface with chemical gradients composed of a mixture of three different metals is reported here for the first time. This proof-of-principle experiment was carried out with bipolar electrochemistry, which takes advantage of the interfacial potential polarization established between an electrolyte solution and a conducting substrate. The latter does act as a bipolar electrode when exposed to an external electric field, thus allowing the concomitant electroreduction of several metal salts at one side of the surface. Three different metals were selected, namely copper, nickel and zinc. Each electrochemical process has a specific energetic requirement depending on the corresponding formal potential. This was demonstrated by changing the applied electric field value and comparing the resulting size of the metal deposit area. At a fixed driving force (*i.e.* fixed value of the applied electric field), copper is deposited on a larger area than nickel, whereas zinc only appears at the very edge of the surface where the polarization potential reaches the highest value. The deposition of bimetallic and trimetallic surface gradients was achieved with a variation of the chemical composition along the surface of the bipolar electrodes. Such surfaces exhibit a complex composition gradient which is ultimately due to a quaternary metal system (gold substrate with copper, nickel and zinc deposits). They could find possible applications in the future as the method allows the single-step preparation of surfaces with a continuous evolution of the nature, composition and thickness of the deposits. The concept can be used to prepare libraries of surface compositions by tuning parameters like the electric field value, the nature and concentration of the metal precursors, the global ionic strength as well as the duration of the deposition.

#### References

- [1] S.O. Krabbenborg, J. Huskens, Electrochemically generated gradients, *Angew. Chem. Int. Ed.* 53 (2014) 9152.
- [2] C. Ulrich, O. Andersson, L. Nyholm, F. Björefors, Formation of molecular gradients on bipolar electrodes, *Angew. Chem. Int. Ed.* 47 (2008) 3034.
- [3] C. Ulrich, O. Andersson, L. Nyholm, F. Björefors, Potential and current density distributions at electrodes intended for bipolar patterning, *Anal. Chem.* 81 (2009) 453.
- [4] S. Inagi, Y. Ishiguro, M. Atobe, T. Fuchigami, Bipolar patterning of conducting polymers by electrochemical doping and reaction, *Angew. Chem. Int. Ed.* 49 (2010) 10136.
- [5] Y. Ishiguro, S. Inagi, T. Fuchigami, Gradient doping of conducting polymer films by means of bipolar electrochemistry, *Langmuir* 27 (2011) 7158.
- [6] S. Inagi, H. Nagai, I. Tomita, T. Fuchigami, Parallel polymer reactions of a polyfluorene derivative by electrochemical oxidation and reduction, *Angew. Chem. Int. Ed.* 52 (2013) 6616.
- [7] F. Mavré, R.K. Anand, D.R. Laws, K.-F. Chow, B.-Y. Chang, J.A. Crooks, R.M. Crooks, Bipolar electrodes: A useful tool for concentration, separation, and detection of analytes in microelectrochemical systems, *Anal. Chem.* 82 (2010) 8766.
- [8] G. Loget, A. Kuhn, Shaping and exploring the micro- and nanoworld using bipolar electrochemistry, *Anal. Bioanal. Chem.* 400 (2011) 1691.
- [9] S.E. Fosdick, K.N. Knust, K. Scida, R.M. Crooks, Bipolar electrochemistry, *Angew. Chem. Int. Ed.* 52 (2013) 10438.
- [10] G. Loget, D. Zigah, L. Bouffier, N. Sojic, A. Kuhn, Bipolar electrochemistry: From materials science to motion and beyond, *Acc. Chem. Res.* 46 (2013) 2513.
- [11] W. Kumsapaya, M.-F. Bakai, G. Loget, B. Goudeau, C. Warakulwit, J. Limtrakul, A. Kuhn, D. Zigah, Janus beads obtained by grafting of organic layers via bipolar electrochemistry, *Chem. Eur. J.* 19 (2013) 1577.
- [12] J.-C. Bradley, J. Crawford, K. Ernazarova, M. McGee, S.G. Stephens, Wire formation on circuit boards using spatially coupled bipolar electrochemistry, *Adv. Mater.* 9 (1997) 1168.
- [13] J.-C. Bradley, H.-M. Chen, J. Crawford, J. Eckert, K. Ernazarova, T. Kurzeja, M. Lin, M. McGee, W. Nadler, S.G. Stephens, Creating electrical contacts between metal particles using directed electrochemical growth, *Nature* 389 (1997) 268.
- [14] J.-C. Bradley, Z. Ma, Contactless electrodeposition of Palladium catalysts, *Angew. Chem. Int. Ed.* 38 (1999) 1663.
- [15] J.C. Bradley, S. Dengra, G.A. Gonzalez, G. Marshall, F.V. Molina, Ion transport and deposit growth in spatially coupled bipolar electrochemistry, *J. Electroanal. Chem.* 478 (1999) 128.
- [16] C. Warakulwit, T. Nguyen, J. Majimel, M.-H. Delville, V. Lapeyre, P. Garrigue, V. Ravaine, J. Limtrakul, A. Kuhn, Dissymmetric carbon nanotubes by bipolar electrochemistry, *Nano Lett.* 8 (2008) 500.
- [17] Z. Fattah, G. Loget, V. Lapeyre, P. Garrigue, C. Warakulwit, J. Limtrakul, L. Bouffier, A. Kuhn, Straightforward single-step generation of microswimmers by bipolar electrochemistry, *Electrochim. Acta* 56 (2011) 10562.
- [18] G. Loget, J. Roche, A. Kuhn, True bulk synthesis of Janus objects by bipolar electrochemistry, *Adv. Mater.* 24 (2012) 5111.
- [19] Z. Fattah, P. Garrigue, V. Lapeyre, A. Kuhn, L. Bouffier, Controlled orientation of asymmetric copper deposits on carbon microobjects by bipolar electrochemistry, *J. Phys. Chem. C* 116 (2012) 22021.
- [20] Z. Fattah, P. Garrigue, B. Goudeau, V. Lapeyre, A. Kuhn, L. Bouffier, Capillary electrophoresis as a production tool for asymmetric microhybrids, *Electrophoresis* 34 (2013) 1985.
- [21] R. Ramaswamy, C. Shannon, Screening the optical properties of Ag-Au alloy gradients formed by bipolar electrodeposition using surface enhanced Raman spectroscopy, *Langmuir* 27 (2011) 878.
- [22] S. Ramakrishnan, C. Shannon, Display of solid-state materials using bipolar electrochemistry, *Langmuir* 26 (2010) 4602.
- [23] N. Dorri, P. Shahbazi, A. Kiani, Self-movement of water droplet at the gradient nanostructure of Cu fabricated using bipolar electrochemistry, *Langmuir* 30 (2014) 1376.
- [24] G. Loget, S. So, R. Hahn, P. Schmuki, Bipolar anodization enables the fabrication of controlled arrays of TiO<sub>2</sub> nanotube gradients, *J. Mater. Chem. A* 2 (2014) 17740.
- [25] G. Loget, G. Larcade, V. Lapeyre, P. Garrigue, C. Warakulwit, J. Limtrakul, M.-H. Delville, V. Ravaine, A. Kuhn, Single point electrodeposition of nickel for the dissymmetric decoration of carbon tubes, *Electrochim. Acta* 55 (2010) 8116.
- [26] G. Loget, A. Kuhn, Propulsion of microobjects by Dynamic bipolar self-regeneration, *J. Am. Chem. Soc.* 132 (2010) 15918.
- [27] B.-Y. Chang, F. Mavré, K.-F. Chow, J.A. Crooks, R.M. Crooks, Snapshot voltammetry using a triangular bipolar microelectrode, *Anal. Chem.* 82 (2010) 5317.
- [28] S. Munktel, M. Tydén, J. Höglström, L. Nyholm, F. Björefors, Bipolar electrochemistry for high-throughput corrosion screening, *Electrochem. Commun.* 34 (2013) 274.
- [29] S. Kong, O. Fontaine, J. Roche, L. Bouffier, A. Kuhn, D. Zigah, Electropolymerization of polypyrrole by bipolar electrochemistry in an ionic liquid, *Langmuir* 30 (2014) 2973.
- [30] J. Roche, G. Loget, D. Zigah, Z. Fattah, B. Goudeau, S. Arbault, L. Bouffier, A. Kuhn, Straight-forward synthesis of ringed particles, *Chem. Sci.* 5 (2014) 1961.
- [31] A. Kuhn, F. Argoul, Revisited experimental analysis of morphological changes in thin-layer electrodeposition, *J. Electroanal. Chem.* 371 (1994) 93.
- [32] N.D. Nikolić, K.I. Popov, Lj. J. Pavlović, M.G. Pavlović, The effect of hydrogen codeposition on the morphology of copper electrodeposits. I. The concept of effective overpotential, *J. Electroanal. Chem.* 588 (2006) 88.
- [33] A. Radisic, P.M. Vereecken, P.C. Searson, F.M. Ross, The morphology and nucleation kinetics of copper islands during electrodeposition, *Surf. Sci.* 600 (2006) 1817.
- [34] S. Song, C.M. Ortega, Z. Liu, J. Du, X. Wu, Z. Cai, L. Sun, *In situ* study of copper electrodeposition on a single carbon fiber, *J. Electroanal. Chem.* 690 (2013) 53.
- [35] G. Loget, J. Roche, E. Gianessi, L. Bouffier, A. Kuhn, Indirect bipolar electrodeposition, *J. Am. Chem. Soc.* 134 (2012) 20033.
- [36] L. Bouffier, A. Kuhn, Design of a wireless electrochemical valve, *Nanoscale* 5 (2013) 1305.